Revealing neutrino mass ordering at the CEPC and FCC-ee

Wei Liu,[1] Supriya Senapati,[1] and Jin Sun[2,*]

[1]*Department of Applied Physics and MIIT Key Laboratory of Semiconductor Microstructure and Quantum Sensing, Nanjing University of Science and Technology, Nanjing 210094, China*

[2]*Particle Theory and Cosmology Group, Center for Theoretical Physics of the Universe, Institute for Basic Science (IBS), Daejeon 34126, Korea*

(Received 21 January 2026; accepted 25 June 2026; published 14 July 2026)

The ordering of neutrino masses remains a key unknown in particle physics and cosmology. While upcoming oscillation experiments are expected to determine the mass ordering at low energies, it is important to explore complementary probes that access the underlying mechanism of neutrino mass generation. In this work, we show that future high-energy electron-positron colliders can provide sensitivity to the neutrino mass ordering through the lepton-flavor structure of heavy neutral lepton (HNL) interactions. In the minimal type-I seesaw scenario with two nearly degenerate HNLs, the flavor composition of the heavy–light neutrino mixings is strongly correlated with the light-neutrino mass spectrum, leading to distinct collider signatures for normal and inverted mass orderings. We demonstrate that future Z factories such as CEPC and FCC-ee can probe these flavor patterns over a wide region of parameter space, establishing collider searches for HNLs as a complementary approach to neutrino mass ordering studies.

DOI: 10.1103/v52b-wsbn

I. INTRODUCTION

Neutrino oscillation experiments [1] allow two possible neutrino mass orderings: the normal hierarchy (NH), $m_3 > m_2 > m_1$, and the inverted hierarchy (IH), $m_2 > m_1 > m_3$, with neutrino masses below the eV scale. Determining the true neutrino mass ordering is a central open question in particle physics, with profound implications for the origin of neutrino mass, neutrinoless double beta decay, and the matter-antimatter asymmetry of the Universe. While upcoming experiments such as JUNO [2], DUNE [3], and Hyper-Kamiokande [4] aim to resolve this question through precision measurements of neutrino oscillations at low energies, complementary probes from other frontiers are equally essential.

Heavy neutral leptons (HNLs), predicted in the type-I seesaw mechanism [5–8], provide a complementary probe of neutrino mass generation at high-energy colliders. These heavy Majorana fermions mix weakly with the active neutrinos, with mixings parametrized by $|U_{\alpha N}|^2$ ($\alpha = e$, μ, τ), and N represents the mass eigenstates of the HNLs. However, existing collider searches mainly focused on single-flavor mixing scenarios, and they are generally insensitive to the neutrino mass ordering [9–34]. In this paper, we show that collider experiments can determine the mass ordering by exploiting the flavor structure of HNL interactions.

To reproduce neutrino oscillation data, at least two HNLs are required. In the minimal seesaw scenario with two nearly degenerate HNLs, the HNL flavor mixings are strongly correlated with the light-neutrino mass spectrum. In particular, the mixings inherit the flavor structure of the heaviest light-neutrino states, leading to a suppressed electron mixing in the NH, $|U_{eN}^2| \ll |U_{\mu N}^2| \sim |U_{\tau N}^2|$, whereas comparable mixings among all flavors are expected in the IH, $|U_{eN}^2| \sim |U_{\mu N}^2| \sim |U_{\tau N}^2|$ [35–39]. Consequently, the comparison of lepton-flavor final states in HNL decays provides a indirect handle on the neutrino mass ordering.

Future Z factories, such as CEPC and FCC-ee, offer an ideal environment to test this idea due to the large statistics of HNLs production. We quantify the sensitivity to the mass ordering in the seesaw parameter space $(m_N, U_{\rm tot}^2)$ and demonstrate that colliders can provide a complementary determination of the mass ordering.

II. LEPTON FLAVOR MIXING OF THE HNL

In the minimal type-I seesaw scenario with two nearly degenerate HNLs N_I ($I = 1, 2$), the heavy-light mixing parameters $\Theta_{\alpha I}$ not only govern the production and decay of HNLs at colliders but also encode the flavor structure

*Contact author: sunjin0810@ibs.re.kr

Published by the American Physical Society under the terms of the Creative Commons Attribution 4.0 International license. Further distribution of this work must maintain attribution to the author(s) and the published article's title, journal citation, and DOI. Funded by SCOAP³.

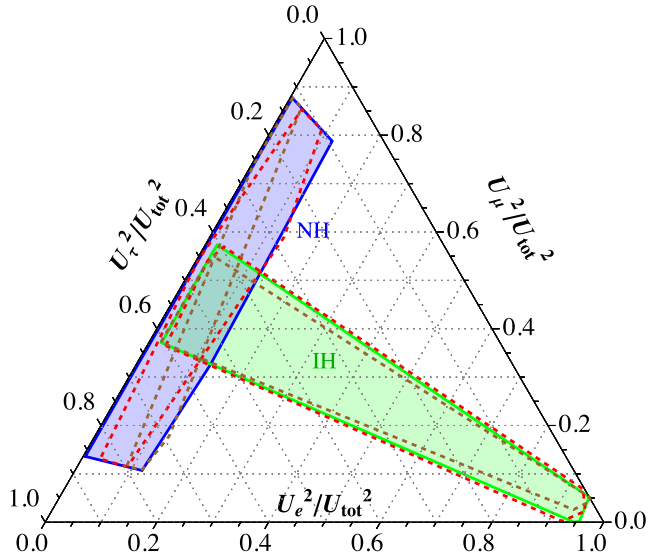


FIG. 1. Ternary plot showing the 3σ allowed region of flavor-mixing ratios $U_\alpha^2/U_{\rm tot}^2$, $\alpha = e, \mu, \tau$ for NH (blue) and IH (green). They are obtained by NuFIT 6.0 [41,42] and JUNO's new result [43]. The dashed red (brown) curve shows the region under the best-fit CP phase from T2K (NOνA), assuming a future uncertainty of 8° (7°) from DUNE + μTHEIA [44].

imprinted by the light-neutrino mass spectrum. As a result, the relative strengths of the HNL couplings to the electron, muon, and tau flavors depend sensitively on the neutrino mass ordering. In particular, the NH predicts a suppressed electron mixing due to the vanishing lightest neutrino mass, whereas the IH leads to a more democratic flavor pattern. This makes the lepton-flavor composition of HNL interactions a sensitive probe of the mass ordering.

The experimentally measurable quantities $U_{\alpha N}^2$ arise from the cumulative effects of both N_1 and N_2, expressed as [40]

$$
\begin{aligned}
U_{\alpha N}^2 &= \sum_I |\Theta_{\alpha I}|^2 = \frac{1}{2m_N}(|c_\alpha^+|^2 x_\omega^2 + |c_\alpha^-|^2 x_\omega^{-2}),\\
\text{NH}: c_\alpha^\pm &= iV_{\alpha 2}^{\rm PMNS}\sqrt{m_2} \pm V_{\alpha 3}^{\rm PMNS}\sqrt{m_3},\\
U_{\rm tot}^2 &= \sum_{\alpha,I} |\Theta_{\alpha I}|^2 = \frac{(m_2+m_3)}{2m_N}(x_\omega^2 + x_\omega^{-2}),\\
\text{IH}: c_\alpha^\pm &= iV_{\alpha 1}^{\rm PMNS}\sqrt{m_1} \pm V_{\alpha 2}^{\rm PMNS}\sqrt{m_2},\\
U_{\rm tot}^2 &= \sum_{\alpha,I} |\Theta_{\alpha I}|^2 = \frac{(m_1+m_2)}{2m_N}(x_\omega^2 + x_\omega^{-2}).
\end{aligned}
\tag{1}
$$

Here, $U_{\alpha N}^2$ and $U_{\rm tot}^2$ quantify the HNL mixing to a particular flavor and three flavors in total, respectively. And the rest of quantities are defined in the Appendix A. Equation (1) shows explicitly that, in the minimal seesaw with two HNLs, the flavor composition of the heavy-light mixing is not arbitrary but is fully determined by the light-neutrino mass spectrum and the Pontecorvo-Maki-Nakagawa-Sakata (PMNS) mixing matrix. Consequently, the HNL flavor ratios provide a direct imprint of the mass ordering.

TABLE I. The range of $U_{\alpha N}^2/U_{\rm tot}^2$ for NH/IH mass orderings.

Mass ordering	$U_{eN}^2/U_{\rm tot}^2$	$U_{\mu N}^2/U_{\rm tot}^2$	$U_{\tau N}^2/U_{\rm tot}^2$
NH	$(3.1\times10^{-3}, 0.14)$	(0.11, 0.88)	(0.09, 0.86)
IH	(0.021, 0.96)	(0, 0.57)	(0, 0.61)

Following Eq. (1), we scan the neutrino oscillation parameters within their 3σ allowed ranges from NuFIT [41,42] and JUNO's latest result [43] to obtain the ternary distributions shown in Fig. 1. In the NH case, the absence of the ν_1 contribution, together with $|V_{e1}^{\rm PMNS}| \gg |V_{e2,3}^{\rm PMNS}|$, leads to a significantly suppressed electron mixing of the HNL. As a result, the allowed range of $U_{eN}^2/U_{\rm tot}^2$ is confined to $(3.1\times10^{-3}, 0.14)$, as summarized in Table I.

Improved precision in neutrino oscillation measurements can further reduce the allowed parameter space. Although JUNO's first results already demonstrate this potential [43], sizable uncertainties remain. Among the oscillation parameters, the Dirac CP phase δ_D is currently the least constrained and exhibits a notable tension between T2K [45] and NOνA [46], with best-fit values of $\delta_D \simeq -\pi/2$ (T2K) and $\delta_D \simeq 148°$ (NOνA).[1] To illustrate its impact, Fig. 1 shows the predicted NH regions corresponding to the best-fit δ_D values from T2K (red dashed) and NOνA (brown dashed), assuming future uncertainties of 8° and 7°, respectively, achievable with DUNE and μTHEIA [44]. In contrast, the IH region remains largely unchanged. This demonstrates that future precision measurements of δ_D will significantly sharpen the HNL flavor predictions.

III. SENSITIVITY ON NEUTRINO MASS ORDERING

The distinct flavor structures of HNL mixings associated with NH and IH provide a novel way to probe the neutrino mass ordering through the lepton-flavor composition of HNL decays at colliders, as discussed below.

To achieve large HNL statistics, we focus on future high-luminosity lepton colliders, in particular the Circular Electron-Positron Collider (CEPC) [48] and the Future Circular Collider in the electron–positron mode (FCC-ee) [49]. Our analysis targets the Z pole, corresponding to a center-of-mass energy of $\sqrt{s} = 91.2$ GeV, with an integrated luminosity of $\mathcal{L} \simeq 200$ ab^{-1}.

The signal process consists of single-HNL production in association with a neutrino or antineutrino, followed by its decay predominantly into a charged lepton and a pair of jets,

$$
e^+e^- \to N\nu(\bar{\nu}), \qquad N \to \ell_\alpha jj, \tag{2}
$$

[1]Recent combined analyses have partially reduced this tension [47].

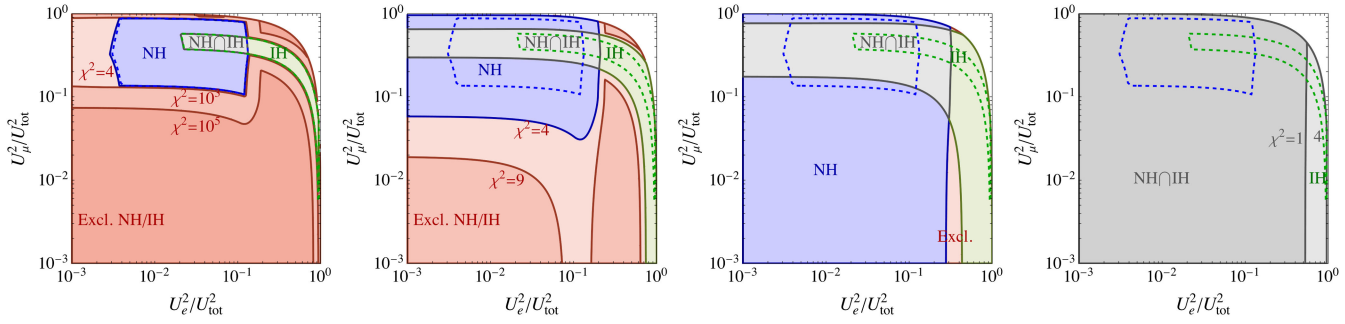


FIG. 2. Sensitivity of the neutrino mass orderings in the plane of $(U^2_{eN}/U^2_{\rm tot}, U^2_{\mu N}/U^2_{\rm tot})$, at $\sqrt{s} = 91.2$ GeV CEPC/FCC-ee with $\mathcal{L} \approx 200$ ab^{-1}, for (a) $U^2_{\rm tot} \approx 10^{-5}$, (b) 10^{-7}, (c) 10^{-8}, and (d) 4×10^{-9}, respectively, when $m_N \sim 50$ GeV.

where $\ell_\alpha = e, \mu$ denotes the charged lepton in the final state. Final states involving τ leptons are neglected due to the limited reconstruction efficiency and larger associated uncertainties. To ensure precise lepton-flavor identification and sufficient event statistics, we focus on prompt HNL decays, requiring the decay length in the laboratory frame to satisfy $L_N \lesssim 1$ mm. Alternative facilities, such as a muon collider [50–52] and μTRISTAN [53], can also probe HNL production. However, for the processes considered here, the corresponding production cross sections are significantly suppressed compared to those at CEPC and FCC-ee. We therefore restrict our collider analysis to electron-positron machines.

Using MG5_aMC@NLO [54], event samples are generated with selection criteria requiring leptons and jets to lie within a pseudorapidity range of $|\eta| < 2.5$ and to satisfy $p_T(j/\ell) > 10$ GeV. The expected number of signal events in each lepton flavor channel is given by

$$N_{S,\alpha} = \sigma(Z) \times \mathrm{Br}(Z \to N\nu(\bar{\nu})) \times \mathrm{Br}(N \to \ell_\alpha jj) \times \mathcal{L} \times \epsilon, \tag{3}$$

where $\mathrm{Br}(Z \to N\nu(\bar{\nu})) \propto U^2_{\rm tot}$ and $\mathrm{Br}(N \to \ell_\alpha jj) \propto U^2_{\alpha N}/U^2_{\rm tot}$. The overall efficiency is factorized as $\epsilon \simeq \epsilon_{\rm prompt} \times \epsilon_{\rm recon}$. The prompt-decay efficiency, $\epsilon_{\rm prompt} \simeq 1 - e^{-l_{\rm dec}/L_N}$, accounts for HNL decays occurring within the primary vertex resolution $l_{\rm dec} \simeq 1$ mm, where the decay length L_N is given in the Appendix A. For electrons and muons, both the CEPC and FCC-ee detectors are designed to achieve near-perfect reconstruction and identification performance. Full detector simulations indicate reconstruction efficiencies exceeding 99% for isolated leptons over a wide angular acceptance [55,56].

Hence, for short-lived HNLs, the number of signal events can be well approximated as

$$N_{S,\alpha} \simeq \mathcal{O}(10^{11}) \times U^2_{\rm tot} \times R_\alpha \equiv N_0 \times R_\alpha, \tag{4}$$

where $R_\alpha \equiv U^2_{\alpha N}/U^2_{\rm tot}$ encodes the flavor composition of the active-sterile mixing and $N_0 \sim \mathcal{O}(10^{11}) \times U^2_{\rm tot}$ denotes the total number of signal events, which is independent of flavor.

The dominant Standard Model background arises from irreducible diboson processes. Applying the same selection criteria, we find

$$N_{B,\alpha} \simeq 1.4 \times 10^5, \tag{5}$$

per flavor for $\alpha = e, \mu$.

To probe the neutrino mass ordering, we analyze the signal and background distributions in the two-flavor plane (R_e, R_μ), which directly maps onto the ternary regions shown in Fig. 1. For a fixed value of $U^2_{\rm tot}$, we define the detection significance as

$$\chi^2_{\rm NH/IH} = \sum_{\alpha=e,\mu} \frac{[N_0(R^{\rm obs}_\alpha - R^{\rm NH/IH}_\alpha)]^2}{N_0 R^{\rm NH/IH}_\alpha + N_{B,\alpha}}, \tag{6}$$

where $R^{\rm obs}_\alpha$ denotes the observed flavor fraction and $R^{\rm NH/IH}_\alpha$ is the theoretical prediction under the normal or inverted mass ordering. Requiring $\min(\chi^2_{\rm NH/IH}) > 4$, we can exclude the NH or IH hypothesis at approximately the 2σ level.

In Fig. 2, we present the sensitivity to the neutrino mass ordering in the (R_e, R_μ) plane for (a) $U^2_{\rm tot} \simeq 10^{-5}$, (b) 10^{-7}, (c) 10^{-8}, and (d) 4×10^{-9}, respectively, assuming $m_N \simeq 50$ GeV. $\chi^2_{\rm NH/IH}$ is evaluated by taking $R^{\rm obs}_\alpha$ to coincide with the coordinates in the (R_e, R_μ) plane, while $R^{\rm NH/IH}_\alpha$ corresponds to the regions predicted for NH (blue dashed) and IH (green dashed) hypotheses.

Following Table II, the figure distinguishes four regions according to their capability to test the NH and IH hypotheses. As $U^2_{\rm tot}$ increases in Fig. 2, the resulting growth in the $\chi^2_{\rm NH/IH}$ leads to three correlated effects: (i) an expansion of the excluded region, (ii) a contraction of the ambiguous region where the NH and IH cannot be distinguished, and (iii) a convergence of the NH- or IH-favored regions toward their respective theoretically predicted parameter spaces. Taken together, these effects

TABLE II. The NH, IH, NH/IH favor and excluded regions in Fig. 2 and their range of $\min(\chi^2_{\rm NH/IH})$.

Region	Color	$\min(\chi^2_{\rm NH})$	$\min(\chi^2_{\rm IH})$
NH favor	Blue	<4	>4
IH favor	Green	>4	<4
NH ∩ IH favor	Gray	<4	<4
Excluded	Red	>4	>4

substantially enhance the discrimination power between the two neutrino mass orderings.

To quantify the overall discrimination power, we define the fraction of parameter space (in $\log_{10}$ scale) for which the neutrino mass ordering can be unambiguously identified,

$$K = 1 - \frac{S_{\rm NH\cap IH}}{S_{\rm tot}}, \tag{7}$$

where $S_{\rm NH\cap IH}$ denotes the area of the region in which both the NH and IH hypotheses are allowed and $S_{\rm tot}$ is the total area spanned by the theoretically predicted NH and IH parameter spaces. The quantity K therefore provides a global measure of the fraction of the allowed seesaw parameter space that permits an unambiguous determination of the neutrino mass ordering, rather than a confidence level associated with a single parameter point.

Owing to the intrinsic overlap between the predicted NH and IH regions, we find $K \lesssim 0.90$ even in the limit of large event statistics. When $N_0 \lesssim 2\sqrt{\sum_{\alpha=e,\mu} N_{B,\alpha}}$, the excluded region disappears, while the overlap region (NH ∩ IH) covers almost the entire parameter space, driving $K \simeq 0$.

In Fig. 3, we show contours of the fraction K in the $(m_N, U^2_{\rm tot})$ plane, together with existing bounds and future sensitivities. Cosmological observations from Planck constrain the sum of light neutrino masses, $\sum_i m_{\nu_i} \simeq U^2_{\rm tot} m_N \lesssim 0.12$ eV, via the seesaw relation [57]. Bounds from charged lepton radiative decays, $\mathrm{Br}(\ell_\alpha \to \ell_\beta\gamma) \propto U^2_\alpha U^2_\beta$, are shown by the black curves for NH (solid) and IH (dashed), with details given in the Appendix A. The CEPC/FCC-ee sensitivity is kinematically suppressed as $m_N \lesssim 70$ GeV, since the two-body phase space suppresses $\Gamma(Z \to N\nu) \propto (1 - m^2_N/m^2_Z)^2$, leaving too few events to determine the neutrino mass ordering.

Although CEPC and FCC-ee cannot directly probe the seesaw limit, they exhibit strong discriminating power for the neutrino mass ordering: $K \simeq 1\%$ for $U^2_{\rm tot} \simeq 4 \times 10^{-9}$, rising to $K \simeq 30\%\,(60\%)$ for $U^2_{\rm tot} \simeq 10^{-8}\,(10^{-7})$. Near-maximal discrimination, $K \simeq 90\%$, as set by current oscillation parameter, can be reached for $U^2_{\rm tot} \gtrsim 10^{-6}$. This is about 1 order of magnitude below existing bounds (red solid line).

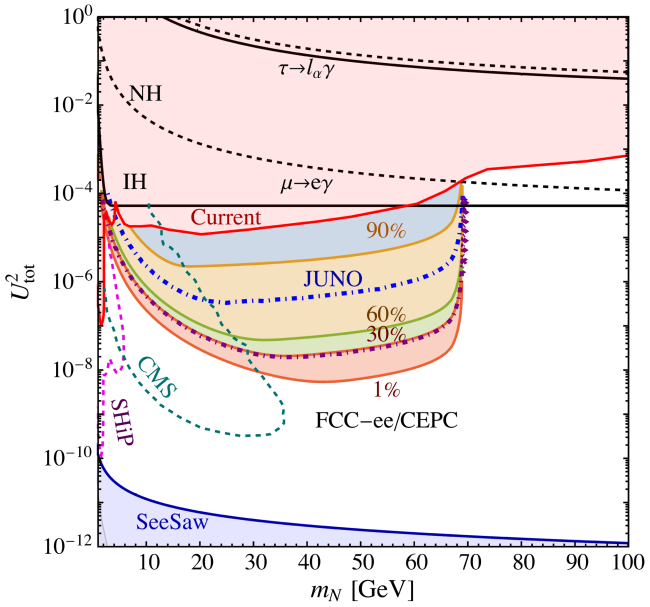


FIG. 3. Fraction of the parameter space (in $\log_{10}$ scale) that allows unambiguous identification of the neutrino mass ordering (NMO) via $e^+e^- \to N\nu(\bar{\nu})$, followed by $N \to \ell_\alpha jj$, at $\sqrt{s} = 91.2$ GeV for CEPC/FCC-ee with $\mathcal{L} \simeq 200$ ab^{-1}. Regions with $K > 1\%$ (30%, 60%, 90%) and $K < 30\%$ (60%, 90%) are shaded in red (green, orange, and cyan), respectively. The red area labeled "current" is excluded by existing constraints [58], while dashed contours labeled "SHiP" and "CMS" indicate future sensitivities [59,60]. The black line denotes the bound from $\ell_\alpha \to \ell_\beta\gamma$, for NH (dashed) and IH (solid). The "seesaw" region reflects the cosmological bound $\sum_i m_{\nu_i} \simeq U^2_{\rm tot} m_N \lesssim 0.12$ eV with $i = 1, 2, 3$ from Planck data [57]. Blue/purple dashed dotted curves are overlaid to show the interplay with JUNO's results for the indication of the physics beyond the two-HNL case with scenario A/B.

IV. INTERPLAY WITH JUNO'S RESULTS

Since JUNO is expected to determine the neutrino mass ordering within the next five years, prior to the completion of future lepton colliders, it is interesting to explore the possible interplay with JUNO's results.

Here, we consider two extreme scenarios to illustrate this interplay to show the best sensitivity of CEPC/FCC-ee to test two-HNL regime, as summarized in Table III. In scenario A, JUNO confirms the NH, while CEPC/FCC-ee have achieved the largest discrimination with only e observation with $R_e = (N_0 + N_{B,e})/(N_0 + \sum N_{B,\alpha})$. To establish this tension at the 2σ level, approximately $N_0 \simeq 3.7 \times 10^3$ events are required.

TABLE III. Scenarios for possible interplay between JUNO and CEPC/FCC-ee to test neutrino mass orderings at 2σ.

Scenario	JUNO	CEPC/FCC-ee
A	NH favor	$R_e = (N_0 + N_{B,e})/(N_0 + \sum N_{B,\alpha})$
B	IH favor	$R_\mu = (N_0 + N_{B,\mu})/(N_0 + \sum N_{B,\alpha})$

In scenario B, JUNO determines the IH. As an extreme case, we assume that CEPC/FCC-ee observes only the muon flavor, which would again be inconsistent with the JUNO result. Similarly, about $N_0 \simeq 8.2 \times 10^4$ events would be needed to reach the 2σ significance. In Fig. 3, the blue and purple dot-dashed curves indicate the regions where such deviations could signal physics beyond the minimal two-HNL framework for scenario A/B.

V. CONCLUSION

In this work, we have shown that the lepton-flavor structure of heavy neutral lepton interactions at future electron-positron colliders provides a sensitive probe of the neutrino mass ordering within the minimal type-I seesaw framework. In scenarios with two nearly degenerate HNLs, the flavor composition of the heavy-light neutrino mixings is tightly correlated with the light-neutrino mass spectrum, leading to characteristic and experimentally testable signatures for normal and inverted orderings.

Focusing on future Z factories such as CEPC and FCC-ee, we demonstrated that measurements of flavor-resolved HNL decays can probe mass-ordering-dependent parameter space over a wide range of HNL masses and mixings. While upcoming oscillation experiments are expected to determine the neutrino mass ordering through precision measurements at low energies, collider-based probes access fundamentally different information by testing the ultraviolet structure of neutrino mass generation. As such, collider measurements offer an independent and complementary validation of the neutrino mass spectrum within the seesaw paradigm.

A consistent picture emerging from both oscillation experiments and collider searches would provide strong evidence for minimal seesaw models with low-scale HNLs. Conversely, any discrepancy between low-energy determinations and collider-based flavor patterns would point to additional dynamics beyond the minimal framework, such as three-HNLs or nonstandard interactions. In particular, once the neutrino mass ordering is determined by JUNO, we show two illustrative scenarios in which the flavor patterns measured at future lepton colliders could be inconsistent with the oscillation results, thereby signaling physics beyond the minimal two-HNL framework. In this sense, collider probes of the HNL flavor structure remain valuable regardless of the experimental timeline for resolving the neutrino mass ordering, and they play a central role in testing the microscopic origin of neutrino masses.

ACKNOWLEDGMENTS

We thank F. F. Deppisch and Chayan Majumdar for useful discussions. W. L. is supported by National Natural Science foundation of China (Grant No. 12205153). J. S. was supported by IBS under Project No. IBS-R018-D1. The authors gratefully acknowledge the valuable discussions and insights provided by the members of the China Collaboration of Precision Testing and New Physics (CPTNP).

DATA AVAILABILITY

The data that support the findings of this article are not publicly available upon publication because it is not technically feasible and/or the cost of preparing, depositing, and hosting the data would be prohibitive within the terms of this research project. The data are available from the authors upon reasonable request.

APPENDIX A: TYPE-I SEESAW FRAMEWORK

We consider a minimal type-I seesaw with two HNLs ν_{RI} ($I = 1, 2$), sufficient to reproduce neutrino oscillation data. The relevant Lagrangian is

$$\mathcal{L} = i\bar{\nu}_{RI}\partial\nu_{RI} - Y_{\alpha I}(\bar{L}_\alpha \cdot \tilde{H})\nu_{RI} - \frac{1}{2}M_I\bar{\nu}^c_{RI}\nu_{RI}, \quad \text{(A1)}$$

where $\alpha = e,\ \mu,\ \tau$ and M_I is taken diagonal. After electroweak symmetry breaking, $m_D = Yv/\sqrt{2}$, and the neutrino mass matrix reads

$$\mathcal{L}^\nu_m = -\frac{1}{2}\begin{pmatrix}\bar{\nu}^c_L & \bar{\nu}_R\end{pmatrix}\begin{pmatrix}0 & m_D^T \\ m_D & m_R\end{pmatrix}\begin{pmatrix}\nu^c_L \\ \nu_R\end{pmatrix}. \quad \text{(A2)}$$

In the seesaw limit $m_D \ll m_R$, the light neutrino mass matrix is $m_\nu \simeq -m_D^T m_R^{-1} m_D$. The flavor eigenstates are related to mass eigenstates by

$$\nu_{L\alpha} = V^{\rm PMNS}_{\alpha i}\nu_i + \Theta_{\alpha I}N^c_I, \qquad \Theta_{\alpha I} \simeq \frac{vY_{\alpha I}}{M_I}. \quad \text{(A3)}$$

We employ the Casas-Ibarra parametrization [61],

$$m_D = iV^{\rm PMNS}\sqrt{m_\nu^{\rm diag}}R\sqrt{m_R^{\rm diag}}, \quad \text{(A4)}$$

with $m_R^{\rm diag} = {\rm diag}(M_1, M_2)$. For normal (inverted) ordering, $m_1 = 0$ ($m_3 = 0$), and the complex orthogonal matrix R is

$$R^{\rm NH} = \begin{pmatrix}0 & 0 \\ \cos\omega & \sin\omega \\ -\sin\omega & \cos\omega\end{pmatrix},$$
$$R^{\rm IH} = \begin{pmatrix}\cos\omega & \sin\omega \\ -\sin\omega & \cos\omega \\ 0 & 0\end{pmatrix}, \quad \text{(A5)}$$

where ω is complex and we define $x_\omega \equiv e^{\mathrm{Im}\,\omega}$. Majorana phases are included through the PMNS matrix.

The charged-current interaction in the mass basis is

$$-\mathcal{L}_{\mathrm{CC}} = \frac{g}{\sqrt{2}} W_\mu^+ \sum_\ell \left(\sum_{i=1}^{3} V_{\ell i}^* \bar{\nu}_i + \sum_{I=1}^{2} \Theta_{\ell I}^* \bar{N}_I^c \right) \gamma^\mu P_L \ell + \mathrm{H.c.} \tag{A6}$$

For $M_1 \simeq M_2$ and $\Theta_{\ell 1} = \pm i \Theta_{\ell 2}$, the two HNLs form a pseudo-Dirac fermion with an approximate $U(1)$ symmetry.

HNLs decay via off-shell W/Z bosons into leptonic and semileptonic final states. The decay length in the laboratory frame is approximately [62]

$$L_N \simeq \frac{1.6}{U_{\mathrm{tot}}^2} \left(\frac{m_N}{\mathrm{GeV}} \right)^{-6} \left(1 - \frac{m_N^2}{m_Z^2} \right) \mathrm{cm}. \tag{A7}$$

Existing constraints on active-sterile mixing are summarized in Ref. [58]. Mixing among different flavors induces radiative decays $\ell_i \to \ell_j \gamma$ at one loop [63,64]. The strongest bound arises from MEG II, $\mathrm{Br}(\mu \to e\gamma) < 1.5 \times 10^{-13}$ [65], with additional limits from $\tau \to \ell\gamma$ searches [66,67]. Future displaced-vertex searches at CMS [60] and the SHiP beam-dump experiment [59,68] provide complementary sensitivity, particularly in the long-lived HNL regime.

APPENDIX B: BACKGROUND AT COLLIDER

The irreducible four-fermion Standard Model background for CEPC and FCC-ee operating at the Z pole, $e^+e^- \to \ell\nu jj$, is generated at leading order using MG5_aMC@NLO. The simulation includes contributions from both associated production via on-shell and off-shell W bosons as well as from Z/γ^* production followed by radiation of an off-shell W from one of the Z decay legs. Other Standard Model backgrounds, including ZZ, WZ, $Z\nu\bar{\nu}$, top-quark, and multiboson processes, are neglected, as they either produce additional visible objects or require misidentification to mimic the exclusive one lepton and two jet final state. The resulting leading-order cross section for the background is found to be 0.72 fb per flavor.

[1] S. Navas *et al.* (Particle Data Group), Review of particle physics, Phys. Rev. D **110**, 030001 (2024).
[2] Z. Djurcic *et al.* (JUNO Collaboration), JUNO conceptual design report, arXiv:1508.07166.
[3] B. Abi *et al.* (DUNE Collaboration), Deep Underground Neutrino Experiment (DUNE), far detector technical design report, volume I introduction to DUNE, J. Instrum. **15**, T08008 (2020).
[4] K. Abe *et al.* (Hyper-Kamiokande Collaboration), Hyper-Kamiokande design report, arXiv:1805.04163.
[5] P. Minkowski, $\mu \to e\gamma$ at a Rate of one out of 10^9 muon decays?, Phys. Lett. B **67**, 421 (1977).
[6] T. Yanagida, Horizontal symmetry and masses of neutrinos, Prog. Theor. Phys. **64**, 1103 (1980).
[7] M. Gell-Mann, P. Ramond, and R. Slansky, Complex spinors and unified theories, Conf. Proc. C **790927**, 315 (1979).
[8] R. N. Mohapatra and G. Senjanovic, Neutrino mass and spontaneous parity nonconservation, Phys. Rev. Lett. **44**, 912 (1980).
[9] K. Kaneta, Z. Kang, and H.-S. Lee, Right-handed neutrino dark matter under the $B-L$ gauge interaction, J. High Energy Phys. 02 (2017) 031.
[10] A. Das, P. S. Bhupal Dev, and C. S. Kim, Constraining sterile neutrinos from precision Higgs data, Phys. Rev. D **95**, 115013 (2017).
[11] A. Das, Y. Gao, and T. Kamon, Heavy neutrino search via semileptonic Higgs decay at the LHC, Eur. Phys. J. C **79**, 424 (2019).
[12] K. Bondarenko, A. Boyarsky, D. Gorbunov, and O. Ruchayskiy, Phenomenology of GeV-scale heavy neutral leptons, J. High Energy Phys. 11 (2018) 032.
[13] D. A. Bryman and R. Shrock, Constraints on sterile neutrinos in the MeV to GeV mass range, Phys. Rev. D **100**, 073011 (2019).
[14] S. Balaji, M. Ramirez-Quezada, and Y.-L. Zhou, *CP* violation and circular polarisation in neutrino radiative decay, J. High Energy Phys. 04 (2020) 178.
[15] W. Liu, K.-P. Xie, and Z. Yi, Testing leptogenesis at the LHC and future muon colliders: A Z' scenario, Phys. Rev. D **105** (2022) 095034.
[16] A. M. Abdullahi *et al.*, The present and future status of heavy neutral leptons, J. Phys. G **50**, 020501 (2023).
[17] Y. Zhang and W. Liu, Probing active-sterile neutrino transition magnetic moments at LEP and CEPC, Phys. Rev. D **107**, 095031 (2023).
[18] D. Barducci, W. Liu, A. Titov, Z. S. Wang, and Y. Zhang, Probing the dipole portal to heavy neutral leptons via meson decays at the high-luminosity LHC, Phys. Rev. D **108**, 115009 (2023).
[19] W. Liu, F. F. Deppisch, and Z. Chen, Testing leptogenesis and seesaw in the $B-L$ model using long-lived particle searches, Phys. Rev. D **110**, 035017 (2024).
[20] W. Liu, S. Kulkarni, and F. F. Deppisch, Heavy neutrinos at the FCC-hh in the $U(1)_{B-L}$ model, Phys. Rev. D **105**, 095043 (2022).
[21] C. Han, T. Li, and C.-Y. Yao, Searching for heavy neutrino in terms of tau lepton at future hadron collider, Phys. Rev. D **104**, 015036 (2021).
[22] A. Das and N. Okada, Bounds on heavy Majorana neutrinos in type-I seesaw and implications for collider searches, Phys. Lett. B **774**, 32 (2017).

[23] A. Maiezza, M. Nemevšek, and F. Nesti, Lepton number violation in Higgs decay at LHC, Phys. Rev. Lett. **115**, 081802 (2015).
[24] F. F. Deppisch, W. Liu, and M. Mitra, Long-lived heavy neutrinos from Higgs decays, J. High Energy Phys. 08 (2018) 181.
[25] J. D. Mason, Time-delayed electrons from Higgs decays to right-handed neutrinos, J. High Energy Phys. 07 (2019) 089.
[26] E. Accomando, L. Delle Rose, S. Moretti, E. Olaiya, and C. H. Shepherd-Themistocleous, Novel SM-like Higgs decay into displaced heavy neutrino pairs in U(1)' models, J. High Energy Phys. 04 (2017) 081.
[27] A. M. Gago, P. Hernández, J. Jones-Pérez, M. Losada, and A. Moreno Briceño, Probing the type I seesaw mechanism with displaced vertices at the LHC, Eur. Phys. J. C **75**, 470 (2015).
[28] J. Jones-Pérez, J. Masias, and J. D. Ruiz-Álvarez, Search for long-lived heavy neutrinos at the LHC with a VBF trigger, Eur. Phys. J. C **80**, 642 (2020).
[29] W. Liu, J. Li, J. Li, and H. Sun, Testing the seesaw mechanisms via displaced right-handed neutrinos from a light scalar at the HL-LHC, Phys. Rev. D **106**, 015019 (2022).
[30] J. Li, W. Liu, and H. Sun, Z' mediated right-handed neutrinos from meson decays at the FASER, Phys. Rev. D **109**, 035022 (2024).
[31] F. F. Deppisch, S. Kulkarni, and W. Liu, Sterile neutrinos at MAPP in the $B-L$ model, 11, 2023, arXiv:2311.01719.
[32] W. Liu, S. Kulkarni, and F. F. Deppisch, Revealing the origin of neutrino masses through displaced shower searches in the CMS muon system, Phys. Rev. D **111**, 093003 (2025).
[33] Z. S. Wang, Y. Zhang, and W. Liu, Searching for heavy neutral leptons coupled to axion-like particles at the LHC far detectors and SHiP, J. High Energy Phys. 01 (2025) 070.
[34] Z. S. Wang, Y. Zhang, and W. Liu, Long-lived sterile neutrinos from an axionlike particle at Belle II, Phys. Rev. D **111**, 035010 (2025).
[35] M. Drewes, B. Garbrecht, D. Gueter, and J. Klaric, Testing the low scale seesaw and leptogenesis, J. High Energy Phys. 08 (2017) 018.
[36] J.-L. Tastet, O. Ruchayskiy, and I. Timiryasov, Reinterpreting the ATLAS bounds on heavy neutral leptons in a realistic neutrino oscillation model, J. High Energy Phys. 12 (2021) 182.
[37] M. Drewes, J. Klarić, and J. López-Pavón, New benchmark models for heavy neutral lepton searches, Eur. Phys. J. C **82**, 1176 (2022).
[38] A. Abada, P. Escribano, X. Marcano, and G. Piazza, Collider searches for heavy neutral leptons: Beyond simplified scenarios, Eur. Phys. J. C **82**, 1030 (2022).
[39] M. Drewes, Y. Georis, J. Klarić, and A. Wendels, On the collider-testability of the type-I seesaw model with 3 right-handed neutrinos, J. High Energy Phys. 03 (2025) 176.
[40] S. Eijima, M. Shaposhnikov, and I. Timiryasov, Parameter space of baryogenesis in the νMSM, J. High Energy Phys. 07 (2019) 077.
[41] I. Esteban, M. C. Gonzalez-Garcia, M. Maltoni, I. Martinez-Soler, J. P. Pinheiro, and T. Schwetz, NuFIT-6.0: updated global analysis of three-flavor neutrino oscillations, J. High Energy Phys. 12 (2024) 216.
[42] I. Esteban, M. C. Gonzalez-Garcia, M. Maltoni, I. Martinez-Soler, J. P. Pinheiro, and T. Schwetz, NuFIT-6.0, http://www.nu-fit.org (2024).
[43] A. Abusleme *et al.* (JUNO Collaboration), First measurement of reactor neutrino oscillations at JUNO, arXiv:2511.14593.
[44] S.-F. Ge, C.-F. Kong, and P. Pasquini, Improving *CP* measurement with THEIA and muon decay at rest, Eur. Phys. J. C **82**, 572 (2022).
[45] K. Abe *et al.* (T2K Collaboration), Measurements of neutrino oscillation parameters from the T2K experiment using 3.6×10^{21} protons on target, Eur. Phys. J. C **83**, 782 (2023).
[46] M. A. Acero *et al.* (NOvA Collaboration), Improved measurement of neutrino oscillation parameters by the NOvA experiment, Phys. Rev. D **106**, 032004 (2022).
[47] S. Abubakar *et al.* (T2K and NOvA Collaboration), Joint neutrino oscillation analysis from the T2K and NOvA experiments, Nature (London) **646**, 818 (2025).
[48] CEPC Study Group, CEPC conceptual design report: Volume 1—accelerator, arXiv:1809.00285.
[49] A. Abada *et al.* (FCC Collaboration), FCC-ee: The lepton collider: Future circular collider conceptual design report volume 2, Eur. Phys. J. Special Topics **228**, 261 (2019).
[50] T. H. Kwok, L. Li, T. Liu, and A. Rock, Searching for heavy neutral leptons at a future muon collider, Phys. Rev. D **110**, 075009 (2024).
[51] P. Li, Z. Liu, and K.-F. Lyu, Heavy neutral leptons at muon colliders, J. High Energy Phys. 03 (2023) 231.
[52] K. Mkekała, J. Reuter, and A. F. Żarnecki, Optimal search reach for heavy neutral leptons at a muon collider, Phys. Lett. B **841**, 137945 (2023).
[53] A. Das, J. Li, S. Mandal, T. Nomura, and R. Zhang, Testing tree level TeV scale seesaw scenarios in μTRISTAN, Phys. Rev. D **112**, 035008 (2025).
[54] J. Alwall, R. Frederix, S. Frixione, V. Hirschi, F. Maltoni, O. Mattelaer, H. S. Shao, T. Stelzer, P. Torrielli, and M. Zaro, The automated computation of tree-level and next-to-leading order differential cross sections, and their matching to parton shower simulations, J. High Energy Phys. 07 (2014) 079.
[55] M. Abbrescia *et al.* (IDEA Study Group), The IDEA detector concept for FCC-ee, arXiv:2502.21223.
[56] X. Ai *et al.*, Flavor physics at the CEPC: A general perspective, Chin. Phys. **49**, 103003 (2025).
[57] N. Aghanim *et al.* (Planck Collaboration), Planck 2018 results. VI. Cosmological parameters, Astron. Astrophys. **641**, A6 (2020); **652**, C4(E) (2021).
[58] P. D. Bolton, F. F. Deppisch, and P. S. Bhupal Dev, Neutrinoless double beta decay versus other probes of heavy sterile neutrinos, J. High Energy Phys. 03 (2020) 170.
[59] S. Alekhin *et al.*, A facility to search for hidden particles at the CERN SPS: The SHiP physics case, Rep. Prog. Phys. **79**, 124201 (2016).

[60] M. Drewes and J. Hajer, Heavy neutrinos in displaced vertex searches at the LHC and HL-LHC, J. High Energy Phys. 02 (2020) 070.

[61] J. A. Casas and A. Ibarra, Oscillating neutrinos and $\mu \to e, \gamma$, Nucl. Phys. **B618**, 171 (2001).

[62] M. Drewes, Distinguishing Dirac and Majorana heavy neutrinos at lepton colliders, Proc. Sci. ICHEP2022 (**2022**) 608 [arXiv:2210.17110].

[63] A. Ibarra, E. Molinaro, and S. T. Petcov, Low energy signatures of the TeV scale see-saw mechanism, Phys. Rev. D **84**, 013005 (2011).

[64] D. N. Dinh, A. Ibarra, E. Molinaro, and S. T. Petcov, The $\mu - e$ conversion in nuclei, $\mu \to e\gamma, \mu \to 3e$ decays and TeV scale see-saw scenarios of neutrino mass generation, J. High Energy Phys. 08 (2012) 125; 09 (2013) 023(E).

[65] K. Afanaciev *et al.* (MEG II Collaboration), New limit on the $\mu^+ \to e^+\gamma$ decay with the MEG II experiment, Eur. Phys. J. C **85**, 1177 (2025).

[66] B. Aubert *et al.* (*BABAR* Collaboration), Searches for lepton flavor violation in the decays $\tau^\pm \to e^\pm\gamma$ and $\tau^\pm \to \mu^\pm\gamma$, Phys. Rev. Lett. **104**, 021802 (2010).

[67] A. Abdesselam *et al.* (Belle Collaboration), Search for lepton-flavor-violating tau-lepton decays to $\ell\gamma$ at Belle, J. High Energy Phys. 10 (2021) 019.

[68] C. Ahdida *et al.* (SHiP Collaboration), Sensitivity of the SHiP experiment to heavy neutral leptons, J. High Energy Phys. 04 (2019) 077.